



ELSEVIER

Available online at [www.sciencedirect.com](http://www.sciencedirect.com)

SCIENCE @ DIRECT®

Nuclear Instruments and Methods in Physics Research B 232 (2005) 244–248

**NIM B**  
Beam Interactions  
with Materials & Atoms

[www.elsevier.com/locate/nimb](http://www.elsevier.com/locate/nimb)

# Potential sputtering and kinetic sputtering from a water adsorbed Si(100) surface with slow highly charged ions

N. Okabayashi <sup>a,\*</sup>, K. Komaki <sup>a</sup>, Y. Yamazaki <sup>a,b</sup>

<sup>a</sup> Institute of Physics, Graduate School of Arts and Sciences, University of Tokyo, 3-8-1 Komaba, Meguro, Tokyo 153-8902, Japan

<sup>b</sup> Atomic Physics Laboratory, RIKEN, 2-1 Hirosawa, Wako, Saitama 351-0198, Japan

Available online 3 May 2005

## Abstract

We measured charge state dependence and incident angle dependence of sputtering yields and two-dimensional (2D) position distributions for  $H^+$ ,  $Si^+$  and  $SiOH^+$  ions emitted from a water adsorbed Si(100) surface irradiated by a few keV  $Ar^{q+}$  ( $q = 4-8$ ). It was found that (1)  $H^+$  yield strongly depended on the charge state and increased with increasing incident angle, (2)  $Si^+$  and  $SiOH^+$  yields were independent of the charge state and increased with increasing incident angle.

© 2005 Elsevier B.V. All rights reserved.

PACS: 79.20.Rf

Keywords: Water; Si(100); Highly charged ions; Potential sputtering; Kinetic sputtering

## 1. Introduction

Sputtering phenomena induced with slow highly charged ions (HCIs) have been intensively studied in the last two decades to search for fundamental sputtering processes and to apply the phe-

nomena to surface analysis and nano-size etching [1,2]. When an HCI approaches and impacts on a surface, atoms and molecules on the surface can be emitted via kinetic as well as via electronic processes due to the strong electric field and large potential energy of the HCI. The former process is called kinetic sputtering (KS) and the latter process is called potential sputtering (PS). The contribution of PS and KS for various materials had been reported by measuring sputtering yields as a function of charge state [3–10]. One of the examples showing dominant contribution of PS is the sputtering from a LiF and  $SiO_2$  irradiated by slow

\* Corresponding author. Present address: Institute of Multi-disciplinary Research for Advanced Materials, Tohoku University, Katahira 2-1-1, Sendai, 980-8577, Japan. Tel.: +81 22 217 5369; fax: +81 22 217 5371.

E-mail address: [norio@radphys4.c.u-tokyo.ac.jp](mailto:norio@radphys4.c.u-tokyo.ac.jp) (N. Okabayashi).

HCI [7,8]. Recently, another sputtering model was proposed for insulating surfaces, where PS was combined with KS leading to effective secondary particle ejection [9].

A typical example showing dominance of PS for a well-defined adsorbate is emission of  $H^+$  from hydrogen terminated Si(100) surfaces irradiated by a few keV  $Xe^{q+}$  ( $q = 4-12$ ). It was reported that the  $H^+$  yield strongly depended on the charge state like  $q^\gamma$  ( $\gamma \approx 5$ ) but was independent of the incident angle [4]. The charge state dependence could be explained by a pair-wise bond-breaking model [11] which had its basis in the classical over-barrier model [12]. In the present work, in order to study further  $H^+$  sputtering process, a water adsorbed Si(100)- $2 \times 1$  surface was adopted. Charge state dependence and incident angle dependence of sputtering yields and two-dimensional (2D) position distributions for  $H^+$ ,  $Si^+$  and  $SiOH^+$  ions are reported.

## 2. Experimental

The experimental setup and data analysis were described in detail elsewhere [13,14] and are only briefly repeated here. HCIs were extracted from a mini-EBIS [15], charge-state selected with a Wien-filter, periodically swept with a deflector to form a pulse train, and guided into a target chamber. A pulsed electron source was also available for electron stimulated desorption (ESD) experiments. Positively charged secondary ions are accelerated normal to the surface by the electric field applied between the target and a grounded mesh in front of the target. After the mesh, secondary ions travel in the field free region and are finally detected by a 2D position sensitive detector which provides information on 2D position and time-of-flight of each secondary ion.

The sample was cut to  $24 \times 14 \text{ mm}^2$  in area from an 0.5 mm thick B-doped Si(100) wafer (orientation accuracy  $\pm 0.5^\circ$ ) with a resistivity of  $18 \Omega \text{ cm}$ . Before insertion into the target chamber, the sample was chemically treated to prepare a thin oxide layer, which protected the Si surface from contamination [16]. After the target chamber reached ultra high vacuum (UHV), the oxide layer

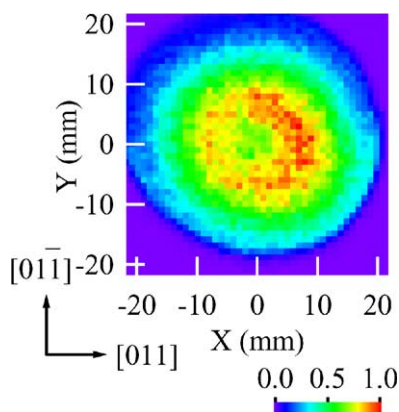


Fig. 1. 2D position distribution of  $H^+$  ions emitted from the  $H_2O/Si(100)$  surface irradiated by 600 eV  $e^-$  with the target biased at 300 V.

was removed by repeated heating as high as 1170 K for three minutes, which formed the Si(100)- $2 \times 1$  reconstructed surface [16]. The Si(100)- $2 \times 1$  surface so prepared was exposed to the residual water molecules.

Fig. 1 shows a 2D position distribution of  $H^+$  ions emitted from the  $H_2O/Si(100)$  surface irradiated by 600 eV electrons, where the target bias is 300 V. In case of ESD, ionized adsorbate is expected to be ejected along the initial bond [17]. The Si(100) surface has two domains, one with its Si dimer bond along  $[011]$  and the other along  $[0\bar{1}1]$ . Each Si atom in the dimer bonds has one dangling bond on which water molecule is dissociatively adsorbed to form Si-H or Si-OH [18,19]. It is known that HCI- or electron-induced emission of  $H^+$  ions dominantly takes place from Si-OH [5,18,19] bond. Although the OH bond has its equilibrium direction along the dimer row [18,20], the torsional vibrational level is rather shallow (e.g.  $70 \text{ cm}^{-1}$  [20]), and as a result, the OH bond may not be fixed along the dimer row at the room temperature. The observed  $H^+$  pattern exhibiting a caldera-shaped pattern (see Fig. 1) is consistent with the above expectation [18,19].

## 3. Results and discussion

Fig. 2 shows charge state dependences of sputtering yields for  $H^+$ ,  $Si^+$  and  $SiOH^+$  ions, which

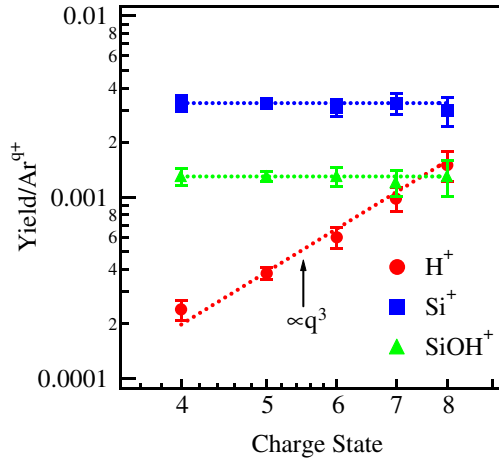


Fig. 2. Charge state dependences of sputtering yields for  $H^+$ ,  $Si^+$  and  $SiOH^+$  ions emitted from the  $H_2O/Si(100)$  surface irradiated by 3.2 keV  $Ar^{q+}$  incident at  $\theta = 30^\circ$ .

were the main species emitted from the  $H_2O/Si(100)$  surface irradiated by 3.2 keV  $Ar^{q+}$  ions ( $q = 4-8$ ) [13]. The incident angle  $\theta$  measured from surface normal is  $30^\circ$ . It is seen that the  $H^+$  yield drastically increases with  $q$  like  $q^\gamma$  ( $\gamma \approx 3$ ), showing the typical feature of PS process. On the other hand, the  $Si^+$  and  $SiOH^+$  yields are independent of  $q$ , showing the characteristic feature of KS process. This sharp contrast between  $H^+$  and  $Si^+$  is similar to the case for  $H/Si(100)$  surface irradiated by a few keV  $Xe^{q+}$  ( $q = 4-12$ ), although  $\gamma \approx 5$  [4]. One of the reasons of this lower value of  $\gamma$  may be the contribution of KS, which was actually observed for  $H^+$  emission from untreated surfaces irradiated by 4.8 keV  $Ar^{q+}$  ( $q = 6-14$ ) [3].

Fig. 3 shows incident angle dependences of sputtering yields for  $H^+$ ,  $Si^+$  and  $SiOH^+$  ions emitted from the  $H_2O/Si(100)$  surface irradiated by 3.2 keV  $Ar^{5+}$  ions. It is seen that the yield of  $H^+$  ions increases with  $\theta$  like  $1/(\cos \theta)^{1.7}$ , which is the typical feature of KS process. This incident angle dependence of  $H^+$  yield is different from that for  $H/Si(100)$  surface irradiated by 4 keV  $Xe^{8+}$ , where  $H^+$  yield is independent of  $\theta$  [4]. The yields of  $Si^+$  and  $SiOH^+$  ions also increased with  $\theta$  like  $1/(\cos \theta)^{1.7}$ , again showing the typical feature of KS process. This observation is the same as the case of  $Si^+$  yield of  $H/Si(100)$  surface irradiated by 4 keV  $Xe^{8+}$  [4].

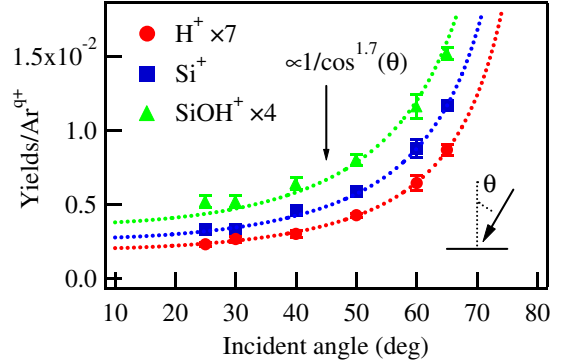


Fig. 3. Incident angle dependences of sputtering yields for  $H^+$ ,  $Si^+$  and  $SiOH^+$  ions emitted from the  $H_2O/Si(100)$  surface irradiated by 3.2 keV  $Ar^{5+}$ .

Fig. 4 shows 2D position distributions of  $H^+$  ions emitted from the  $H_2O/Si(100)$  surface irradiated by (a) 1.2 keV  $Ar^{3+}$  and (b) 1.2 keV  $Ar^{6+}$  for  $\theta = 40^\circ$  and a target bias of 600 V. The origin of the spatial coordinates of the distribution was determined at the center of  $F^+$  distributions [14] of contaminant F atoms on the same surface, assuming  $F^+$  distributions were not disturbed by the KS process very much. It is seen that the distribution for  $Ar^{3+}$  impact consists of a single peak shifted along the  $[0\bar{1}\bar{1}]$  direction which coincides with the direction of incident beam. This observation indicates that the KS process plays some roles in addition to the PS process. The shift of the proton distribution for  $Ar^{6+}$  impact is less than that

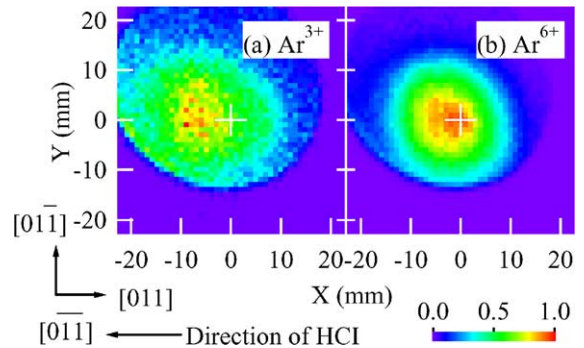


Fig. 4. 2D position distributions of  $H^+$  ions emitted from the  $H_2O/Si(100)$  surface irradiated by (a) 1.2 keV  $Ar^{3+}$  and (b) 1.2 keV  $Ar^{6+}$ , with the incident angle of  $40^\circ$  and the target bias of 600 V. The  $[0\bar{1}\bar{1}]$  direction is identical with the direction of incident beam.

for  $\text{Ar}^{3+}$  impact, indicating the relative contribution of PS process gets more important than the case of  $\text{Ar}^{3+}$ .

Fig. 5 shows the 2D position distributions of  $\text{H}^+$  ions emitted from the  $\text{H}_2\text{O}/\text{Si}(100)$  surface irradiated by 1.8 keV  $\text{Ar}^{6+}$  incident at (a)  $\theta = 29^\circ$  and (b)  $\theta = 47^\circ$ , where the target bias is 400 V. It is seen that the peak position is shifted along the  $[0\bar{1}\bar{1}]$  direction as the incident angle increases, which shows that the KS process plays some role on the proton emission.

Fig. 6 shows 2D position distributions of (a)  $\text{Si}^+$  ions and (b)  $\text{SiOH}^+$  ions emitted from the  $\text{H}_2\text{O}/\text{Si}(100)$  surface irradiated by 1.8 keV  $\text{Ar}^{6+}$  inci-

dent at  $\theta = 47^\circ$ , where the target bias is 400 V. It is seen that the 2D distribution of  $\text{Si}^+$  has a tail toward the downstream of Ar ions, which extends further when the incident angle increases, although the peak appears at normal direction to the surface almost independently of the incident angle. On the other hand, the 2D distribution of  $\text{SiOH}^+$  does not have such a long tail but the peak position is shifted toward the downstream of Ar ions. These observations indicate that  $\text{Si}^+$  and  $\text{SiOH}^+$  ions are both preferentially sputtered toward the downstream of Ar ions, which are at least qualitatively consistent with the feature of KS process.

#### 4. Conclusion

In the present paper, charge state dependence and incident angle dependence of sputtering yields and 2D position distributions for  $\text{H}^+$ ,  $\text{Si}^+$  and  $\text{SiOH}^+$  ions emitted from the  $\text{H}_2\text{O}/\text{Si}(100)$  surface were reported. It was shown for a few keV  $\text{Ar}^{q+}$  ( $q = 4-8$ ) impact that (1) the emission of  $\text{H}^+$  ions had the features of PS process and KS process, (2)  $\text{Si}^+$  and  $\text{SiOH}^+$  ions were ejected dominantly by KS process.

#### Acknowledgements

We are deeply indebted to K. Ueda, T. Komeda and S. Fukatsu for their valuable advice, particularly on the sample preparation. Thanks are also due to K. Kuroki for the discussion on the physical processes and the advice on the experimental setup.

#### References

- [1] A. Arnau et al., Surf. Sci. 27 (1997) 113.
- [2] T. Schenkel, A.V. Hamza, A.V. Barnes, D.H. Schneider, Prog. Surf. Sci. 61 (1999) 23.
- [3] N. Kakutani, T. Azuma, Y. Yamazaki, K. Komaki, K. Kuroki, Nucl. Instr. and Meth. B 96 (1995) 541.
- [4] K. Kuroki, N. Okabayashi, H. Torii, K. Komaki, Y. Yamazaki, Appl. Phys. Lett. 81 (2002) 3561.
- [5] K. Kuroki, K. Komaki, Y. Yamazaki, Nucl. Instr. and Meth. B 203 (2003) 183.

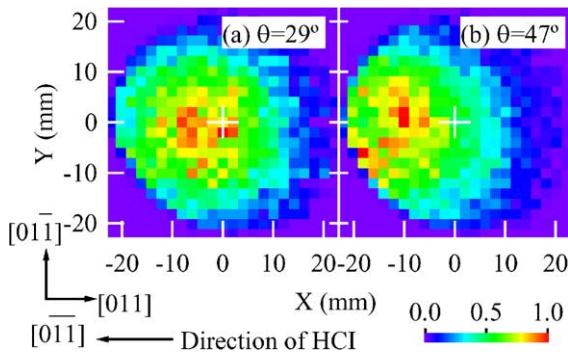


Fig. 5. 2D position distributions of  $\text{H}^+$  ions emitted from the  $\text{H}_2\text{O}/\text{Si}(100)$  surface irradiated by 1.8 keV  $\text{Ar}^{6+}$  incident at (a)  $\theta = 29^\circ$  and (b)  $\theta = 47^\circ$ , with the target bias of 400 V. The  $[0\bar{1}\bar{1}]$  direction is identical with the direction of incident beam.

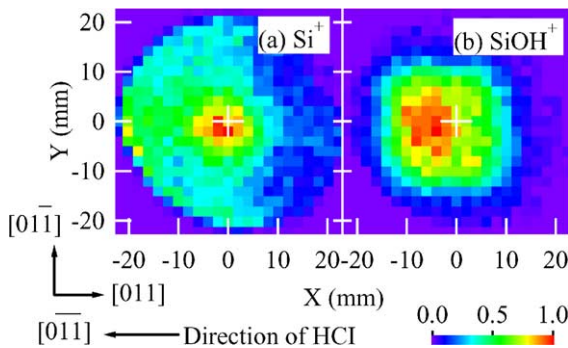


Fig. 6. 2D position distributions of (a)  $\text{Si}^+$  ions and (b)  $\text{SiOH}^+$  ions emitted from the  $\text{H}_2\text{O}/\text{Si}(100)$  surface irradiated by 1.8 keV  $\text{Ar}^{6+}$  incident at  $\theta = 47^\circ$ , with the target bias of 400 V. The  $[0\bar{1}\bar{1}]$  direction is identical with the direction of incident beam.

- [6] S.T. de Zwart, T. Fried, D.O. Boerma, R. Hoekstra, A.G. Drentje, A.L. Boers, *Surf. Sci.* 177 (1986) L939.
- [7] T. Neidhart, F. Pichler, F. Aumayr, H.P. Winter, M. Schmid, P. Varga, *Phys. Rev. Lett.* 74 (1995) 5280.
- [8] M. Sporn, G. Libiseller, T. Neidhart, M. Schmid, F. Aumayr, H.P. Winter, P. Varga, M. Grether, D. Niemann, N. Stolterfoht, *Phys. Rev. Lett.* 79 (1997) 945.
- [9] G. Hayderer et al., *Phys. Rev. Lett.* 86 (2001) 3530.
- [10] T. Schenkel, A.V. Hamza, A.V. Barnes, D.H. Schneider, J.C. Banks, B.L. Doyle, *Rev. Lett.* 81 (1998) 2590.
- [11] J. Burgdörfer, Y. Yamazaki, *Phys. Rev. A* 54 (1996) 4140.
- [12] J. Burgdörfer, P. Lerner, F.W. Meyer, *Phys. Rev. A* 44 (1991) 5674.
- [13] N. Okabayashi, K. Komaki, Y. Yamazaki, *Nucl. Instr. and Meth. B*205 (2003) 725.
- [14] N. Okabayashi, K. Komaki, Y. Yamazaki, *Nucl. Instr. and Meth. B*, in press, doi:10.1016/j.nimb.2005.03.220.
- [15] K. Okuno, *Jpn. J. Appl. Phys.* 28 (1989) 1124.
- [16] A. Ishizaka, Y. Shiraki, *J. Electrochem. Soc.* 133 (1986) 666.
- [17] D. Ramsier, J.T. Yates Jr., *Surf. Sci. Rep.* 12 (1991) 243.
- [18] C.U.S. Larsson, A.L. Johnson, A. Flodström, T.E. Madey, *J. Vac. Sci. Technol. A* 5 (1987) 842.
- [19] Q. Gao, Z. Dohnalek, C.C. Cheng, W.J. Choyke, J.T. Yates Jr., *Surf. Sci.* 312 (1994) 261.
- [20] R. Konecny, D.J. Doren, *J. Chem. Phys.* 106 (1997) 2426.